

efficiently construct multiple layered-3D hepatic structures. Interestingly, we found that mimicking the 3D hepatic structure not only assists the iHeps to stably repopulate, but also enhanced hepatic gene expression profiles of iHeps.

Conclusions: Combining 3D bioprinting technology with iHep generation protocol may be a realistic option for overcoming the problems including donor shortage and surgical complications of liver transplantation, and thereby offers a new paradigm in the field of liver regenerative medicine.

Fibrosis and regeneration

PS-071

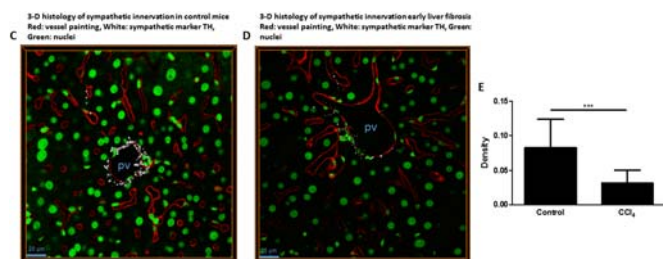
3-D imaging of the hepatic sympathetic innervation and its neuroplasticity in early liver fibrosis

J.-C. Lin¹, S.-C. Tang², H.-S. Lee³, S.-J. Peng². ¹Division of Gastroenterology and Hepatology, Department of Internal Medicine, Tri-Service General Hospital, National Defense Medical Center, Taipei; ²Institute of Biotechnology, National Tsing Hua University, Hsinchu; ³Department of Pathology and Laboratory Medicine, Kaohsiung Veterans General Hospital, Kaohsiung, Taiwan
E-mail: doc10506@gmail.com

Background and Aims: Liver receives extensive sympathetic innervation to regulate hepatic microcirculation, glycogen and lipid metabolism, liver repair and regeneration, circadian rhythms, and biliary function. Moreover, adrenergic innervation can enhance liver fibrosis. However, details of the intrahepatic sympathetic innervation and its plasticity in response to fibrogenesis remains incompletely defined because standard histology cannot provide a global view of the innervation. Here, we prepared transparent liver specimens to investigate the spatial features of the intrahepatic sympathetic innervation and its neuroplasticity in early fibrogenesis.

Methods: Cardiac perfusion of fluorescent lectin was used to label hepatic blood vessels. Tyrosine hydroxylase with nuclear counterstaining was used to reveal sympathetic nerve fibers and microstructures. Optical-clearing solution was applied to enable 3-dimensional confocal microscopy of liver microarchitecture to visualize the intrahepatic sympathetic innervation. Early liver fibrosis was induced by injection of carbon tetrachloride in adult mice.

Results: Optical clearing of the mouse liver specimen (Figure 1) was efficient to establish the 3-dimensional imaging and illustration of intrahepatic microstructures and sympathetic innervation with micrometer-level resolution (Figure 2). In the early liver fibrosis, we observed sympathetic neuroplasticity in response to the injury (Figure 3).



Conclusions: This liver histological approach provides a useful tool for 3-D image of sympathetic nerve fibers to better characterize their roles in early liver fibrosis. Furthermore, anatomical and functional studies on other neural pathways (including cholinergic nerves, peptidergic nerves, and nitrenergic nerves) will be examined in different diseased liver by this established platform.

PS-072

Relaxin-coated superparamagnetic iron-oxide nanoparticles as a novel theranostic approach for the diagnosis and treatment of liver fibrosis

R. Bansal¹, B. Nagórniewicz¹, G. Storm^{1,2}, J. Prakash¹. ¹Targeted Therapeutics, Department of Biomaterials, Science and Technology, University of Twente, Enschede; ²Department of Pharmaceutics, Utrecht University, Utrecht, The Netherlands
E-mail: R.bansal@utwente.nl

Background and Aims: Hepatic fibrosis is a growing health problem with no effective and clinically approved therapy. Hepatic stellate cells (HSCs) are the key cells involved in the pathogenesis of liver fibrosis. Upon activation, HSCs are transformed into contractile ECM-producing myofibroblasts leading to scar tissue formation. HSCs contraction contributes significantly to the portal hypertension thereby further impairing the liver function. Relaxin (RLN) has been shown to inhibit HSC activation and contraction thereby ameliorate liver fibrosis and portal hypertension. However, RLN has very poor pharmacokinetics and frequent administration can lead to detrimental side effects e.g. vasodilation. Therefore, we aimed to develop a nanoparticle-based delivery system to improve pharmacokinetic and therapeutic efficacy of RLN for the diagnosis and treatment of liver fibrosis.

Methods: We conjugated RLN to PEGylated iron oxide nanoparticles (RLN-MNP) and characterized the size, charge and stability. We examined relaxin conjugation and HSCs binding/uptake. We analyzed RXFP1 receptor expression on activated HSCs, CCl₄-induced liver fibrosis mouse models and human liver cirrhosis tissues using quantitative PCR and immunohistochemistry. Thereafter, we assessed the effects of RLN-MNP on human HSCs *in-vitro* and on CCl₄-induced advanced liver fibrosis mouse model *in-vivo*.

Results: RLN-MNP was synthesized and RLN conjugation was confirmed. RLN-MNP showed specific binding and uptake to TGFβ-activated human HSCs. *In-vitro*, RLN-MNP and unconjugated RLN significantly inhibited TGFβ-induced 3D-collagen gel contraction and HSCs migration suggesting that RLN-MNP retained RLN binding and effects after conjugation. We found significant up-regulation of RXFP1 in TGFβ-activated HSCs and CCl₄-induced liver fibrosis mouse model. *In-vivo* in established chronic liver fibrosis mouse model, both RLN and RLN-MNP strongly attenuated fibrosis by inhibiting HSC activation, ECM deposition and angiogenesis. Importantly, RLN-MNP but not unconjugated RLN increased Nitric oxide (NO) release by significant up-regulation of iNOS indicating inhibition of portal hypertension. On the other hand, unconjugated RLN induced systemic side effects by inducing systemic NO release (in serum) while RLN-MNP did not. MNP alone did not show any effect *in-vitro* and *in-vivo*.

Conclusions: This study presents a novel strategy to deliver relaxin specifically to HSCs, key pathogenic cells involved in liver fibrogenesis, for the diagnosis and treatment of liver fibrosis.

PS-073

Visualizing hepatocellular amino acid kinetics through mass spectrometry imaging of stable isotopes

M. Arts^{1,2}, Z. Soons¹, L.J. Dubois³, K.A. Pierzchalski², S.R. Ellis², B. Balluff², G.B. Eijkel², T. Cramer⁴, N. Lieuwes³, S.M. Agten⁵, T.M. Hackeng⁵, L.J. van Loon⁶, R.M. Heeren², S.W. Olde Damink¹. ¹General Surgery, NUTRIM, Maastricht University; ²Maastricht Multimodal Molecular Imaging Institute (M4I), Maastricht University; ³Radiation Oncology (Maastro), GROW, Maastricht University, Maastricht, The Netherlands; ⁴General, Visceral and Transplantation Surgery, University Hospital RWTH Aachen, Aachen, Germany; ⁵Biochemistry, CARIM, Maastricht University; ⁶Human Biology and Movement Sciences, NUTRIM, Maastricht University, Maastricht, The Netherlands
E-mail: martijn.arts@maastrichtuniversity.nl

ORAL PRESENTATIONS

Background and Aims: Mass Spectrometry Imaging (MSI) is a high-performance analytical tool that can be used to simultaneously explore the distribution of numerous molecules throughout tissues. Currently, the major limitation is that it provides a static snapshot of what are inherently highly dynamic systems where new molecules are constantly synthesized and consumed. Here we developed new and innovative MSI methodologies that overcome this limitation and simultaneously view the dynamic molecular-level changes occurring within biological tissues by measuring dilution and hydroxylation of stable isotopes. We evaluated the method specifically on hepatocellular metabolism of the essential amino acid L-phenylalanine. Stable isotopes of phenylalanine are commonly used in clinical studies to measure protein turnover. In liver, phenylalanine is hydroxylated into L-tyrosine, and altered levels are related to NASH, NAFLD, cirrhosis and several cancer types. We investigated reproducibility of the measurement of phenylalanine kinetics in liver and correlated kinetics with tissue morphology and other amino acids.

Methods: A bolus injection of $^{13}\text{C}_6$ phenylalanine was administered via the tail vein of immune-compromised Nu-Fox1nu/nu mice ($n = 16$). The mice were sacrificed at 10, 30 or 60 minutes after injection. Liver sections were covered with TAHS for on-tissue derivatization and DHB as a matrix for high resolution MALDI-MSI in positive mode. A novel MATLAB algorithm was developed to visualize spatial tracer kinetics. After MSI analysis, liver sections were stained with hematoxylin and eosin, reviewed for tissue morphology, and co-registered with the Mass Spectrometry images.

Results: We have optimized a method for on tissue derivatization of amino acids and other compounds containing an amine group, facilitating the spatial and dynamic measurement of liver metabolism. We detected and identified ~50 amino metabolites at each pixel. In addition, tracer-tracee ratios and *de novo* hydroxylation were visualized at a spatial resolution of 25 μm . We validated and complemented our results using conventional GC-C-IRMS facilitating quantitative measurement of phenylalanine and tyrosine enrichment of free amino acids and proteins in tissues and blood.

Conclusions: We present a novel and reproducible method to explore the spatial distribution and dynamics of hepatocellular amino acid metabolism, allowing for the first time, visualization of co-localization of phenylalanine and amino acid kinetics in liver.

PS-074

Towards clinical use of targeted therapies for liver fibrosis: development of a sustained release formulation for therapeutic proteins

F. Van Dijk^{1,2}, N. Teekamp², L. Beljaars¹, E. Post¹, D. Schuppan^{3,4}, Y.O. Kim³, K. Poelstra¹, E. Frijlink², W. Hinrichs², P. Olinga².

¹Pharmacokinetics, Toxicology and Targeting; ²Pharmaceutical Technology and Biopharmacy, University of Groningen, Groningen, The Netherlands; ³Institute of Translational Immunology and Research Center for Immune Therapy, Johannes Gutenberg University, Mainz, Germany; ⁴Beth Israel Deaconess Medical Center, Harvard Medical School, Boston, United States

E-mail: fransien.van.dijk@rug.nl

Background and Aims: Active liver fibrosis is characterized by progressive production of extracellular matrix proteins by myofibroblasts, finally leading to cirrhosis. Apart from liver transplantation as the only curative option for decompensated cirrhosis, effective antifibrotic therapy could either halt progression to cirrhosis or induce fibrosis reversal. Many new antifibrotics have low bioavailability. Therefore, we attempt to design a patient friendly drug delivery system, targeting the platelet-derived growth factor β receptor (PDGFR), which is highly upregulated on activated myofibroblasts, for the sustained controlled release of proteinaceous drugs. We developed polymeric microspheres containing the drug carrier pPB-HSA, composed of multiple PDGFR-recognizing peptide moieties (pPB) coupled to human serum albumin (HSA), ensuring

gradual protein release up to at least 7 days. We determined the pharmacokinetic release profile of pPB-HSA in the Mdr2^{-/-} mouse model for liver fibrosis.

Methods: Biodegradable polymeric microspheres containing pPB-HSA were produced by W/O/W emulsification with polymers composed of poly ϵ -caprolactone, poly ethylene glycol and poly L-lactic acid, and characterized with scanning electron microscopy and laser diffraction. The *in vitro* release was measured by an in-house sandwich ELISA. Mdr2^{-/-} mice aged 11–15 weeks, with advanced biliary fibrosis, were injected subcutaneously with microspheres containing 5% protein, and were sacrificed after 1, 3, 5 or 7 days. Plasma and organs were analyzed for the presence of pPB-HSA.

Results: The microspheres had a median size of 23 μm and released pPB-HSA *in vitro* up to at least 14 days. The injected microspheres remained subcutaneous and still contained protein after 7 days. pPB-HSA was released from the microspheres into plasma up to day 7 and reached a steady state concentration of 45 ± 5 ng/ml within 1 day after injection. We confirmed *in vivo* that Mdr2^{-/-} livers exhibited high PDGFR-expression especially on the portal myofibroblasts. Well in line with the PDGFR-expression, pPB-HSA was delivered to the fibrotic livers from day 1 to 7.

Conclusions: The drug carrier pPB-HSA was released from the subcutaneous microspheres into the plasma and could be detected in the fibrotic livers, associated with increased PDGFR-expression, up to 7 days after injection. This study demonstrates that sustained controlled release formulations for proteinaceous drugs constitute a realistic option for long-term treatment of chronic diseases such as fibrosis.

PS-075

The bile acid receptor TGR5 regulates paracellular permeability and protects the liver through an impact on the tight junction protein JAM-A

G. Merlen^{1,2}, J. Ursic-Bedoya^{1,2}, N. Kahale^{1,2,3}, H. Simerabet^{1,2}, I. Doignon^{1,2}, Z. Tanfin^{1,2}, N. Péan^{1,2}, J. Gautherot^{1,2}, C. Ullmer⁴, L. Humbert^{3,5}, D. Rainteau^{3,5}, D. Cassio^{1,2}, T. Tordjmann^{1,2}. ¹U1174, INSERM; ²Université Paris-Sud, Orsay; ³Université Pierre et Marie Curie, Paris, France; ⁴Innovation Center, Roche, Basel, Switzerland; ⁵U1057, INSERM, Paris, France

E-mail: GREGORY.MERLEN@GMAIL.COM

Background and Aims: TGR5, the bile acid (BA) G-protein-coupled receptor protects the liver against BA overload, although through unknown mechanisms. Preliminary data suggested that TGR5, highly expressed in biliary epithelial cells, may regulate biliary epithelium permeability.

Methods: Trans-epithelial resistance (TER) and 10 kDa fluorescent dextran transfer were measured in the NRC (Normal Rat Cholangiocyte) cell line. To study biliary epithelial permeability *in vivo*, fluorescent dextran or modified glycocholic acid were injected in the gallbladder (GB) lumen and traced (spectrofluorimetry and Mass Spectrometry) in plasma and liver. Cells and mice were treated with RO5527239, a specific TGR5 agonist, and with taurochenodeoxycholic acid (TLCA). TGR5-induced signaling pathways were studied by western blot (WB). Tight junction (TJ) proteins expression was investigated by qPCR, WB and immunofluorescence in NRC, in livers and GB from WT (Wild Type) and TGR5-KO mice, under vehicle or TGR5 agonist treatment, in basal conditions or after Bile Duct Ligation (BDL).

Results: In NRC, TGR5 agonists increased TER, reduced dextran passage, induced ERK phosphorylation and EGFR transactivation. Inhibition of EGFR transactivation suppressed TGR5 agonists' effect on NRC paracellular permeability. BA and dextran transepithelial transfer after GB injection was increased in TGR5-KO as compared with WT mice. In TGR5-KO mice, among the TJ proteins studied, only junctional adhesion molecule A (JAM-A) expression and localization at TJ were reduced in bile ducts and GB epithelia, as compared with WT. *In vitro*, TGR5 agonists induced JAM-A expression and

phosphorylation in NRC cells. In TGR5-transfected cells, increasing JAM-A expression correlated with increasing TGR5 expression and TER. *In vivo*, JAM-A phosphorylation was induced in GB epithelium after GB lumen TGR5 agonist injection, in WT but not TGR5-KO mice. After TGR5 agonist treatment, JAM-A expression and phosphorylation increased (biliary tract) and dextran transepithelial transfer decreased (GB injection) in WT but not TGR5-KO mice. After BDL (24–48 h), JAM-A expression and phosphorylation was increased in bile ducts and GB epithelia as compared with control animals, and TGR5 agonist-pre-treated mice were protected from BDL-induced liver injury.

Conclusions: The BA receptor TGR5 regulates biliary epithelial permeability *in vitro* and *in vivo*, through mechanisms modulating the TJ protein JAM-A expression and phosphorylation, thereby protecting liver parenchyma against bile leakage.

PS-076

The I148M PNPLA3 variant is a novel key player modulating the proinflammatory and profibrogenic phenotype of human hepatic stellate cells

F.V. Bruschi¹, T. Claudel¹, M. Tardelli¹, A. Caligiuri², T.M. Stulnig³, F. Marra², M. Trauner¹. ¹Department of Gastroenterology and Hepatology, Internal Medicine III, Medical University of Vienna, Vienna, Austria; ²Clinical Pathophysiology Department, Medical University of Florence, Florence, Italy; ³Christian Doppler-Laboratory for Cardio-Metabolic Immunotherapy and Clinical Division of Endocrinology and Metabolism, Medical University of Vienna, Vienna, Austria
E-mail: francesca.bruschi@meduniwien.ac.at

Background and Aims: The genetic polymorphism of the human PNPLA3 gene I148M is strongly associated with hepatic steatosis and its progression toward non-alcoholic steatohepatitis (NASH), fibrosis and cirrhosis. Hepatic stellate cells (HSC) are key players of liver fibrosis, therefore we aim to explore our hypothesis that PNPLA3 may directly impact on human HSC activation and hepatic fibrogenesis.

Methods: Primary human HSC were isolated, sorted and characterized in two groups, according to the different PNPLA3 genotype (WT = wild type, I148M = allele variant). We generated stably over-expressing WT and I148M LX-2 cells. Moreover we studied PNPLA3 localization and tissue expression in healthy and NASH liver specimen.

Results: Transcriptional and translational levels of PNPLA3 increases during primary human HSC activation. Conversely, transient transfection with siRNA targeting PNPLA3 (knockdown ~70%) significantly decreased the pro-fibrogenic marker α -SMA by 50% ($p < 0.05$). *In line*, immunofluorescence staining revealed co-localization of PNPLA3 and α -SMA in human NASH liver. Compared to PNPLA3 WT cells, untreated HSCs carrying the I148M PNPLA3 variant displayed significantly higher expression of proinflammatory cytokines, such as CCL5 and GM-CSF by 15-fold ($p < 0.01$) and 5-fold ($p < 0.001$) respectively, which also significantly enhanced macrophages migration by 50% ($p < 0.05$). Primary I148M HSCs showed reduced retinol ($p < 0.001$), but higher lipid droplets (LDs) content ($p < 0.001$). *In line*, LX-2 stably overexpressing I148M recapitulated the profibrogenic phenotype observed in primary I148M HSCs and abolished RXR/RAR transcriptional activities. Since PPAR γ is known to antagonize the activation of HSCs, we explored PPAR γ expression and functionality in cells stably expressing the PNPLA3 isoforms. Despite normal PPAR γ ligands abundance, its transcriptional activity was lowered in I148M expressing cells due to Serine84 phosphorylation. The c-Jun kinase (JNK) activity increased 2.5-fold in I148M overexpressing cells ($p < 0.05$), thus inhibiting PPAR γ while promoting AP-1 transcription. Moreover, AP-1 promoter binding was decreased by 60% using specific JNK inhibitors in cells carrying the PNPLA3 variant ($p < 0.01$).

Conclusions: Collectively our data show that PNPLA3 is required for HSC activation and its genetic variant I148M potentiates pro-inflammatory and profibrogenic features of activated HSCs by JNK

mediated phosphorylation of PPAR γ , which leads to higher AP-1 signaling and cytokine production in HSC thus promoting fibrosis development.

PS-077

The purinergic receptor P2X4 regulates liver fibrogenesis

C.L. Guilcher^{1,2,3}, I. Garcin^{1,3}, A. Tebbi^{1,3}, I. Doignon^{1,3}, T. Tordjmann^{1,3}, B. Julien^{1,3}. ¹U 1174, INSERM, Orsay; ²Université Pierre et Marie Curie, Paris; ³Université Paris Sud, Orsay, France
E-mail: camille.le-guilcher@inserm.fr

Background and Aims: Extracellular adenosine triphosphate (ATP) and its receptors constitute a powerful signaling network during tissue remodeling and inflammatory processes. All cell types, under diverse physical or chemical stimuli, can release ATP in the extracellular medium in autocrine or paracrine manners. ATP can bind to membrane purinergic receptors ("P2" receptors) to elicit a wide array of biological responses. All liver cell types express purinergic receptors including P2X (ionotropic) and P2Y (metabotropic) subtypes. In the liver, beside hepatocytes, P2X4 receptor (P2X4R) is highly expressed in Kupffer cells and myofibroblasts (hMF), two key players in hepatic fibrogenesis processes. Importantly, the impact of P2X4R in liver pathophysiology remains unknown. In this work we analyzed P2X4R involvement after bile duct ligation (BDL)-induced fibrosis.

Methods: *In vivo*, after BDL in WT and P2X4KO mice, cytokines (Monocyte chemotactic protein 1, Interleukin-6, Tumor necrosis factor alpha) were quantified by qPCR in the liver and by Luminex in plasma. Liver fibrosis markers were analyzed by qPCR and staining (alpha smooth muscle actin (aSMA), Matrix Metalloproteinases (MMPs), Tissue Inhibitor Metalloproteinases 1 (TIMP1), Transforming growth factor beta, Cytokeratin-19, and Collagen). *In cultured* hMF isolated from WT and P2X4KO mice and from human liver, the impact of P2X4R stimulation by ATP or inactivation by siRNA was studied on the expression of: MMPs (zymography), TIMP1, Collagen type I, aSMA and Interleukin-6 (Western Blot, qPCR). Finally, we studied hMF proliferation, adhesion (immunostaining), contraction (gel contraction assay), and migration (wound healing assay).

Results: After BDL, as compared to WT, P2X4KO mice exhibited significantly less fibrosis, hMF accumulation, pro-fibrogenic and pro-inflammatory markers. *In cultured* P2X4KO hMF, profibrogenic markers were downregulated as compared to WT, which could explain reduced fibrosis in P2X4KO mice. Importantly, P2X4KO hMF displayed lower aSMA protein expression in association with reduced contractile, migrative, adhesive and proliferative properties. Moreover, P2X4 gene extinction (siRNA) in WT hMF and human hMF resulted in a reduction of aSMA protein, thus suggesting that P2X4R may control hMF activation state.

Conclusions: The inactivation of P2X4R protects liver from chronic injury through the modulation of hMF activation and inflammatory response, suggesting that P2X4R may be a new therapeutic target during liver fibrotic diseases.

PS-078

Hepatocyte polyploidy in response to loss of Cdk1 induces chronic hepatic inflammation and progenitor cell activation

M. Dewhurst¹, N.V. Hul¹, M. Caldez¹, P. Kaldis¹. ¹Institute of Molecular and Cell Biology, Singapore, Singapore
E-mail: mattr.dewhurst@gmail.com

Background and Aims: Cyclin-dependent kinase 1 (Cdk1) is essential for mitotic division and germline knockout of Cdk1 is embryonic lethal. Deletion of Cdk1 in hepatocytes (Cdk1^{liv-/-}) does not impair regenerative capacity of the liver however, untreated Cdk1^{liv-/-} animals display extensive hepatic inflammation and fibrosis. We aimed to determine the mechanisms during Cdk1^{liv-/-} development that maintain liver size and function in the absence of hepatocyte proliferation since deregulation of these mechanisms may contribute to the observed pathology.

ORAL PRESENTATIONS

Methods: Cdk1^{liv-/-} livers were collected for IHC, IF and western blotting from two, four, six and eight week old mice. Hepatocytes were isolated from perfused livers for FACS analysis.

Results: Two week-old Cdk1^{liv-/-} livers displayed giant hepatocytes with enlarged nuclei, absent of mitotic markers (H3pS10), and increased fibrotic deposition. FACS analysis of hepatocyte DNA content showed several rounds of endoreplication (<64n).

Hepatocytes increased in size with age and developed multiple yH2AX⁺ nuclear foci. At six weeks, 82% of Cdk1^{liv-/-} hepatocytes stained PCNA⁺ compared to 17% of control hepatocytes. RNAseq analysis indentified an upregulated subset of fetal oncogenes associated with liver progenitor cells. In addition, small hepatocytes staining SOX9⁺ were observed by IF. No evidence of senescence (SAβGal) or necrosis was detected, with only minor increases in apoptotic markers.

Elevated levels of TGFβ mRNA were observed at eight weeks, which correlated with increased Col1a1 expression and extent of fibrosis. Levels of CD8⁺ T cells were also elevated at this time point.

Prolonged depletion of hepatic macrophages by clodronate injections between four and six weeks resulted in a partial reversion of fibrosis and phenotypic severity. Interestingly, the Cdk1^{liv-/-} phenotype appears to be fully resolved after 12 months.

Conclusions: Endoreplication in Cdk1^{liv-/-} hepatocytes results in polyploidic, enlarged cells which maintain liver mass in the absence of proliferation, despite accumulation of extensive DNA damage. Re-emergence of SOX9⁺ hepatocytes suggest that a threshold of DNA re-replication, or DNA damage accumulation, is reached leading to hepatocyte repopulation driven by progenitor cells and/or hepatocyte dedifferentiation. These data suggest an intrinsic ability for hepatocytes to deal with blockade of cell division. However, this comes at the cost of increased inflammation and fibrosis which therapies targeting hepatocyte division should consider.

Portal hypertension and hepatic encephalopathy

PS-079

A new screening strategy for varices by liver and spleen stiffness measurement (LSSM) in cirrhotic patients: a randomized controlled trial

G.L.-H. Wong¹, R. Kwok¹, A.J. Hui², H.L. Chan¹, V.W. Wong¹.

¹Medicine and Therapeutics, The Chinese University of Hong Kong, Hong Kong; ²Medicine, Alice Ho Miu Ling Nethersole Hospital, Tai Po, Hong Kong, China

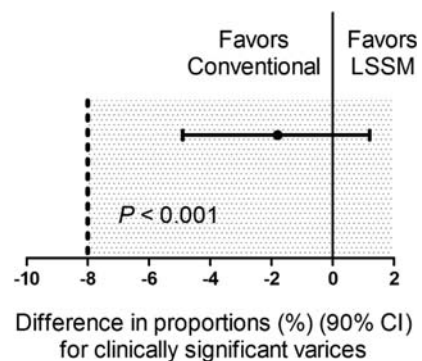
E-mail: wonglaihung@cuhk.edu.hk

Background and Aims: Variceal bleeding is a common and life-threatening complication in patients with liver cirrhosis. Screening with upper endoscopy is recommended but is uncomfortable for patients. Non-invasive assessment with transient elastography for liver/spleen stiffness measurement (LSM and SSM) is accurate in detecting varices. We aimed to test the hypothesis that a new screening strategy for varices guided by LSM and SSM results (LSSM-guided) is non-inferior to universal endoscopic screening in detecting clinically significant varices in patients with cirrhosis.

Methods: This was a non-inferiority, open-label, randomized controlled trial in two hospitals in Hong Kong. Adult patients with known chronic liver diseases, radiological evidence of liver cirrhosis and compensated liver function. The primary outcome was clinically significant varix diagnosed with upper endoscopy. Patients randomized to LSSM arm would first undergo transient elastography examination; those with high LSM (≥ 12.5 kPa) or SSM (≥ 41.3 kPa) results would then proceed to upper endoscopy examination for to

screen varices. On the other hand, patients randomized into control arm would directly undergo upper endoscopy examination.

Results: Between October 2013 and June 2016, 548 patients were randomized to LSSM arm (n = 274) and conventional arm (n = 274) which formed the intention-to-test (ITT) population. Patients in both study arms were predominantly middle-aged men with hepatitis B-related cirrhosis. Around 30% of patients had splenomegaly. Among 264 patients who attended transient elastography examinations, LSM and SSM value was 14.0 ± 9.6 kPa and 37.5 ± 20.7 kPa respectively. In the ITT analysis, 11/274 participants in the LSSM arm (4.0%) and 16/274 in the conventional arm (5.8%) were found to have clinically significant varices. The difference between two groups was -1.8% (90% CI, -4.9% to 1.2% , $P < 0.001$). 51/274 participants in the LSSM arm (18.6%) and 67/274 in the conventional arm (24.5%) were found to have any varices ($P = 0.12$). Hypoalbuminemia, splenomegaly and high SSM but not LSM were independently associated with clinically significant varices.



Conclusions: LSSM-guided screening strategy is non-inferior to the convention approach to detect clinically significant varices. This approach should be recommended to patients with liver cirrhosis (ClinicalTrials.gov: NCT02024347).

PS-080

Simvastatin ameliorates the sinusoidal microcirculatory phenotype, fibrosis and portal hypertension in aged cirrhotic rats

R. Maeso-Diaz^{1,2}, M. Ortega-Ribera¹, A. Fernandez-Iglesias^{1,3}, L. Muñoz^{3,4}, S. Vila^{1,3}, A. Albillos^{3,4}, J.C. Garcia-Pagan^{1,3}, J. Bosch^{1,3}, J. Gracia-Sancho^{1,3}. ¹Liver Vascular Biology Lab, Barcelona Hepatic Hemodynamic Team - IDIBAPS Biomedical Research Institute; ²Medical School, Universitat de Barcelona, Barcelona; ³CIBEREHD; ⁴Gastroenterology and Hepatology, IRYCIS - Universidad de Alcalá, Madrid, Spain

E-mail: jgracia@clinic.ub.es

Background and Aims: We have recently demonstrated the impact of aging on the pathophysiology of chronic liver disease (CLD). Compared to young cirrhotic rats, aged animals with cirrhosis exhibit global exacerbation of the disease due to an aggravation in the phenotype of hepatic sinusoidal cells and hepatocytes. In the last decades, the beneficial effects of statins have been evaluated in young cirrhotic animals, although the mean age of cirrhotic patients has increased. The present study evaluated the effects of simvastatin in an aged cirrhotic model, experimental procedure closer to the real clinical practice.

Methods: 20 month-old cirrhotic rats received simvastatin (5 mg/kg/day) or vehicle for 15 days. Liver microcirculatory phenotype and function was assessed by means of hemodynamic studies (portal pressure-PP, portal blood flow-PBF, hepatic vascular resistance-HVR), hepatic endothelial function (dose-response to acetylcholine), and molecular data: sinusoidal phenotype markers in liver tissue and in freshly isolated liver sinusoidal endothelial cells (LSEC) and hepatic stellate cells (HSC). Moreover, bacterial translocation was evaluated in mesenteric lymph nodes and faecal bacterial load.